

Global fits for the spectral index of the cosmological curvature perturbation

Laura Covi¹ and David H. Lyth^{2★}

¹*DESY Theory Group, Notkestrasse 85, D-22603 Hamburg, Germany*

²*Physics Department, Lancaster University, Lancaster LA1 4YB*

Accepted 2001 February 28. Received 2001 February 5; in original form 2000 September 22

ABSTRACT

Best-fitting values of the spectral index of the curvature perturbation are presented, assuming the Λ CDM cosmology. Apart from the spectral index, the parameters are the Hubble parameter, the total matter density and the baryon density. The data points are intended to represent all measurements that are likely to affect the result significantly. The cosmic microwave anisotropy is represented by the *COBE* normalization, and heights of the first and second peaks are given by the latest Boomerang and Maxima data. The slope of the galaxy correlation function and the matter density contrast on the $8 h^{-1} \text{Mpc}$ scale are each represented by a data point, as are the expected values of the Hubble parameter and matter density. The ‘low-deuterium’ nucleosynthesis value of the baryon density provides a final data point, the fit giving a value higher by about one standard deviation. The reionization epoch is calculated from the model by assuming that it corresponds to the collapse of a fraction $f \gtrsim 10^{-4}$ of matter. We consider the case of a scale-independent spectral index, and also the scale-dependent spectral index predicted by running mass models of inflation. In the former case, the result is compared with the prediction of models of inflation based on effective field theory, in which the field value is small on the Planck scale. A detailed comparison is made with other fits, and other approaches to the comparison with theory.

Key words: cosmic microwave background – cosmology: theory – early Universe – large-scale structure of Universe.

1 INTRODUCTION

The spectral index n , giving the scale dependence of the spectrum $\mathcal{P}_{\mathcal{R}}$ of the primordial curvature perturbation, will be a powerful discriminator between models of inflation when it is accurately determined. Just before the release of the latest Boomerang (de Bernardis et al. 2000) and Maxima data (Hanany et al. 2000) on the cosmic microwave background (CMB) anisotropy, we reported (Lyth & Covi 2000) a global fit to the key pieces of available data. We considered the case of a practically scale-independent spectral index, comparing the best-fitting value with some models of inflation based on effective field theory. We went on to consider the running mass models, corresponding to a spectral index with strong scale dependence, and demonstrated that such scale dependence was allowed by the data.

In the present paper, we update the fit by including the Boomerang and Maxima results for the height of the second peak of the CMB anisotropy, taking the height of the first peak from the same source for consistency. The best-fitting values of the spectral

index and other parameters are different from the previous case, but not dramatically so, while the value of χ^2 , though higher, is still acceptable. We consider, in some detail, the implication of our results for some models of inflation based on effective field theory, drawing a distinction between such models and ad hoc parametrizations of the potential. In the running mass model, the data still allow a strong scale-dependence of the spectral index.

As with our previous fit, we assume the Λ CDM cosmology, in which the Universe is flat and the dark matter is cold. Flatness is the naive prediction of inflation, and there is presently no firm motivation for considering modifications of the simplest dark-matter hypothesis. The model, then, consists of the Λ CDM cosmology, the assumption that a Gaussian primordial curvature perturbation is the only one, and the assumption about reionization that we shall discuss shortly.

2 THE FIT

The fit minimizes χ^2 with the assigned error bars. The data set is the one given in the first two rows of Table 1, plus the accurate value provided by *Cosmic Background Explorer (COBE)* at the

★E-mail: d.lyth@lancaster.ac.uk

Table 1. Fit of the Λ CDM model to presently available data, assuming reionization when a fraction $f = 10^{-2.2}$ of matter has collapsed. (Corresponding redshift at best fit is $z_R = 18$.) The scale-independent spectral index n is a parameter of the model, and so are the next three quantities. Every quantity except n is a data point, with the value and uncertainty listed in the first two rows. The result of the least-squares fit is given in lines three to five. All uncertainties are at the nominal 1σ level. The total χ^2 is 6.3 with three degrees of freedom.

	n	$\Omega_B h^2$	Ω_0	h	$\bar{\Gamma}$	$\bar{\sigma}_8$	$\sqrt{C_{\ell}^{1st}}$	$C_{\ell}^{2nd}/C_{\ell}^{1st}$
Data	–	0.019	0.35	0.65	0.23	0.56	74.0 μ K	0.38
Error	–	0.002	0.075	0.075	0.035	0.059	5 μ K	0.06
Fit	0.987	0.021	0.38	0.62	0.19	0.56	70.8 μ K	0.49
Error	0.051	0.002	0.06	0.05	–	–	–	–
χ^2	–	0.9	0.2	0.2	1.3	0.002	0.4	3.3

relevant scale k_{COBE} ,¹

$$\frac{2}{5} \mathcal{P}_{\mathcal{R}}^{1/2}(k_{COBE}) = 1.94 \times 10^{-5}. \quad (1)$$

This data set is the same as that of the earlier fit, except that the height of the first peak is now taken from the Boomerang/Maxima data, and the ratio of second to first peak height from the same source is now included. For both peaks, we used the pair of data points nearest to the expected peak position, one point from each of the two data sets. The random and systematic errors for each point were added in quadrature, and then the weighted average was taken. The theoretical peak heights in both cases were taken from the output of the CMBfast package (CMBfast 2000; see CMBfast website, <http://physics.nyu.edu/matiasz/CMBFAST/cmbfast.html>), linearly interpolated as described earlier (Lyth & Covi 2000) for the first peak.

Ours is the first fit that takes account of both Boomerang and Maxima data, and which at the same time is global in that there is an attempt to include in some form all data that are likely to constrain the model significantly.² Apart from the CMB data, we include the summaries of data on the galaxy correlation function and the cluster abundance provided by the quantities $\bar{\Gamma}$ and $\bar{\sigma}_8$, admittedly subjective estimates of Ω_0 and h [based on observations (Bahcall et al. 1999; Turner 1999; Freedman 2000) that have nothing to do with the large-scale structure], and the ‘low-deuterium’ nucleosynthesis estimate of the baryon density (Sarkar 1999; Olive, Steigman & Walker 2000).³ We recognize, of course, that our choice of data points and error bars is subjective. For one thing, much of the uncertainty is systematic making the minimization of χ^2 not strictly justified. For another, the device of representing many different measurements by a single error bar loses information. In particular, we have dropped measurements of the CMB anisotropy away from the first and second peaks (which are included for instance by Tegmark, Zaldarriaga & Hamilton 2001). Nevertheless, it seems reasonable to us to prefer some kind of global fit over fits that arbitrarily keep only selected pieces of information such as, for instance, the CMB anisotropy. Moreover, as can be seen from Fig. 1, we can to some extent justify our procedure a posteriori observing that our best-fitting results are

giving a good interpolation also of the CMB data that we are neglecting (in the second peak region our fit is out by two standard deviations, but the situation does not become worse as one moves away from the peak): this is surely not a chance, but is due to the fact that the Λ CDM model gives a good account of the shape of the peaks, thus the most important constraint comes indeed from the peak heights.

Before describing our results, we want to describe our treatment of the reionization redshift z_R . Previously reported fits regard z_R as a parameter, either to be fixed at some reasonable value, or to be included in the fit. We prefer an estimate of z_R provided by the Λ CDM model itself. Apart from maintaining information which is otherwise lost, the use of this estimate will lead to a more realistic lower bound on n . The estimate is obtained by assuming that reionization occurs when some fraction $f \ll 1$ of the matter has collapsed into gravitationally bound structures, for which the epoch can be estimated from the Press–Schechter approximation. We have considered values of f in the reasonable range (Liddle & Lyth 1995) $-4.4 < \log_{10} f < 0$, and the result is shown in the right-hand panel of Fig. 2.⁴ When f decreases over this range, the value of z_R corresponding to the best fit increases from 10 to 26. For comparison, we show in the left-hand panel of Fig. 2 the result with z_R fixed at various values. Over the range $10 < z_R < 26$, the upper bound on n is similar to the one which fixes f (at the value reproducing z_R at best fit). In contrast, the lower bound on n depends strongly on z_R , but relatively weakly on f . The reason is that with fixed f in our adopted range, low values of n give low values of z_R . At the same time, the dependence of our result on the assumption concerning reionization is not entirely insignificant (representative cases are given in the panels of Fig. 3, along with some theoretical predictions that we shall discuss later).

Taking the central value of $f = 10^{-2.2}$, the best-fitting parameters are shown in Table 1. The calculated data points are all within one standard deviation or so of their observed values, except for the height of the second peak relative to that of the first, which is high by almost two standard deviations, and the χ^2 per degree of freedom is still perfectly reasonable. The calculated CMB anisotropy is compared with the full Boomerang/Maxima data set in Fig. 1, where the spectrum of the primordial curvature perturbation is also shown.

We have also investigated the effect of omitting part of our data set. First, we omitted the data point for $\Omega_B h^2$ (coming from nucleosynthesis), and found a best-fitting value of $\Omega_B h^2 \approx 0.29$ in qualitative agreement with the other analyses (Jaffe et al. 2001;

¹ This value has a slight Ω_0 dependence which we include. The small uncertainty is ignored, because including the *COBE* normalization in the fit results in values practically indistinguishable from the central one.

² After the original version of this paper appeared in the archive, a more-or-less global fit did appear (Tegmark et al. 2001), which will be discussed later.

³ The alternative ‘high-deuterium’ estimate corresponds to a much lower baryon density, which is not favoured by the Boomerang/Maxima data.

⁴ The result for $10^{-1} < f < 1$ is not shown, because in the approximation that we are using (Lyth & Covi 2000) it is the same as for the case $f = 10^{-1}$.

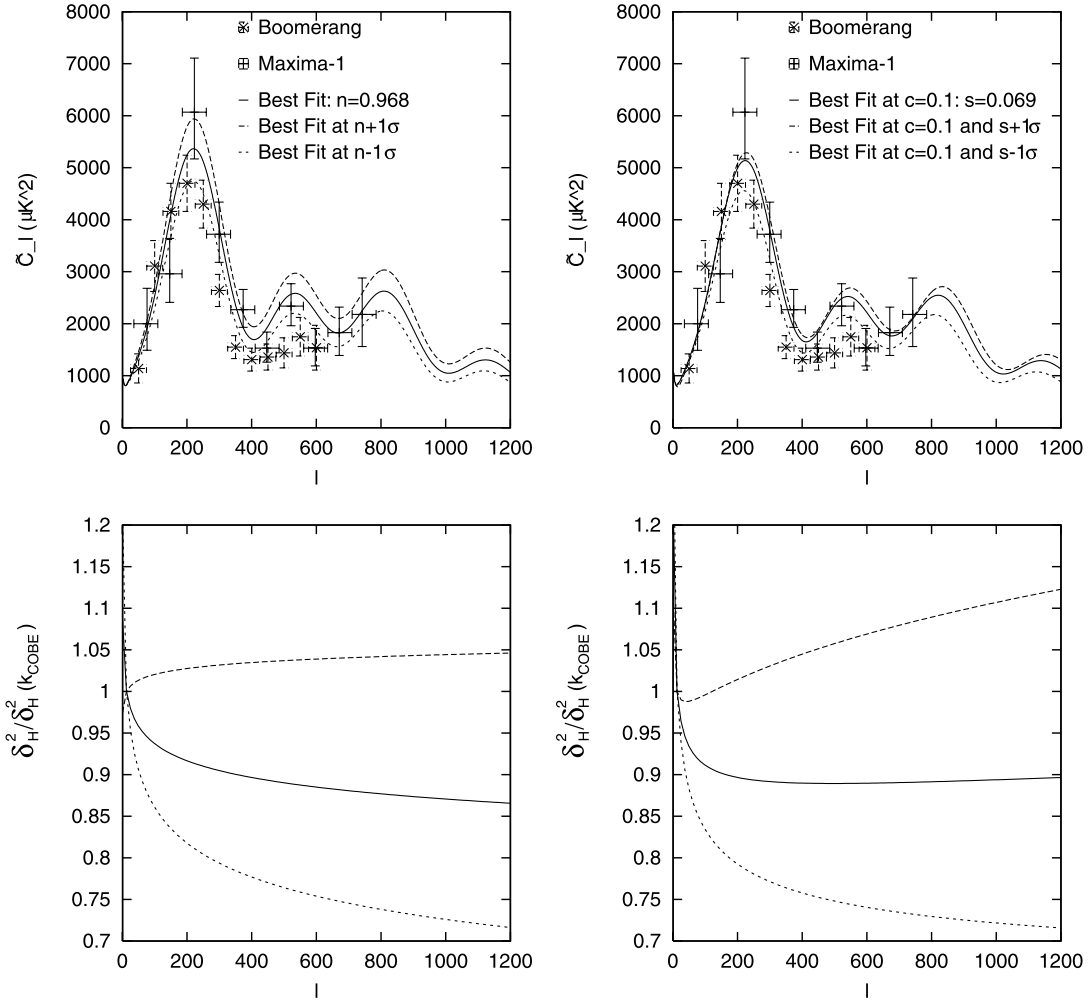


Figure 1. Curves correspond to best fit of $\pm 1\sigma$ for $f \approx 1$. The top panels show the CMB anisotropy \tilde{C}_ℓ , for the case of scale-independent spectral index (left panel) and for the running mass model with a coupling $c = 0.1$ (right panel). The error bars do not include systematic errors; considering these as the calibration uncertainties, they are 20 per cent for Boomerang and 8 per cent for Maxima. The fit used only the two data points nearest to each of the peaks (one each from Boomerang and Maxima) and added the systematic errors in quadrature. Other data sets around the first peak (not shown) span a wider range and their rejection in favour of Boomerang/Maxima is somewhat subjective. The bottom panels show the corresponding spectrum of the primordial curvature perturbation, normalized to 1 at the *COBE* scale, against the scale $\ell(k)$ probed by the CMB anisotropy. The shortest scale shown (biggest ℓ) corresponds to $k^{-1} \approx 10 h^{-1}$ Mpc, at which the galaxy data $\bar{\sigma}_8$ and $\bar{\Gamma}$ apply.

Tegmark et al. 2001). This is five standard deviations higher than our data point, which in our view means that the fit is of little interest. Secondly, we omitted h and/or Ω_0 . Omitting just one of them makes little difference, because their best-fitting values are strongly correlated, but omitting both of them again leads to values very far from the expectation ($\Omega_0 \approx 0.7$ and $h \approx 0.45$) so then this fit too is of little interest.

Finally, we investigated the effect of omitting either one or both the large-scale structure data points, $\bar{\Gamma}$ and $\bar{\sigma}_8$. Eliminating both leads to best-fitting values for $\bar{\Gamma}$ and $\bar{\sigma}_8$ which are respectively three and four standard deviations below the data. Here again, we consider that such a fit is of little interest. [For the record, the fit gives $n = 0.89 \pm 0.07$, in qualitative agreement with another analysis (Kinney, Melchiorri & Riotto 2001).] Omitting just one of them makes little difference to the fit, because they are again strongly correlated. In particular, lowering n lowers both the magnitude of the spectrum on the relevant scales (measured by $\bar{\sigma}_8$) and its slope (measured by $\bar{\Gamma}$).

Our fit is similar to another one (Tegmark et al. 2001, hereafter TZH00). As mentioned already, TZH01 include all the CMB data, whereas we use only the heights of the two peaks plus the *COBE* normalization. On the other hand, our analysis is arguably more complete in two other respects. First, the TZH01 data set did not include $\bar{\sigma}_8$ (nor any other constraint on the normalization of the spectrum in the regime of the large-scale structure), while it replaced our $\bar{\Gamma}$ by a fit to the shape of the galaxy correlation function from a recent infrared survey (Saunders et al. 2000). Secondly, that analysis leaves the reionization redshift as a free parameter, which according to our observations makes the best-fitting value practically zero. The best fit of TZH01 gives a spectral index $n = 0.91 \pm 0.05$ (1σ) to be compared with our $z_R = 0$ result $n = 0.95 \pm 0.03$, with the other parameters similar to ours. Using the best-fitting parameters of TZH01, we find $\bar{\Gamma} = 0.17$ and $\bar{\sigma}_8 = 0.48$, both significantly lower than the data points we assigned to these quantities. We believe that this is the main reason for the lower

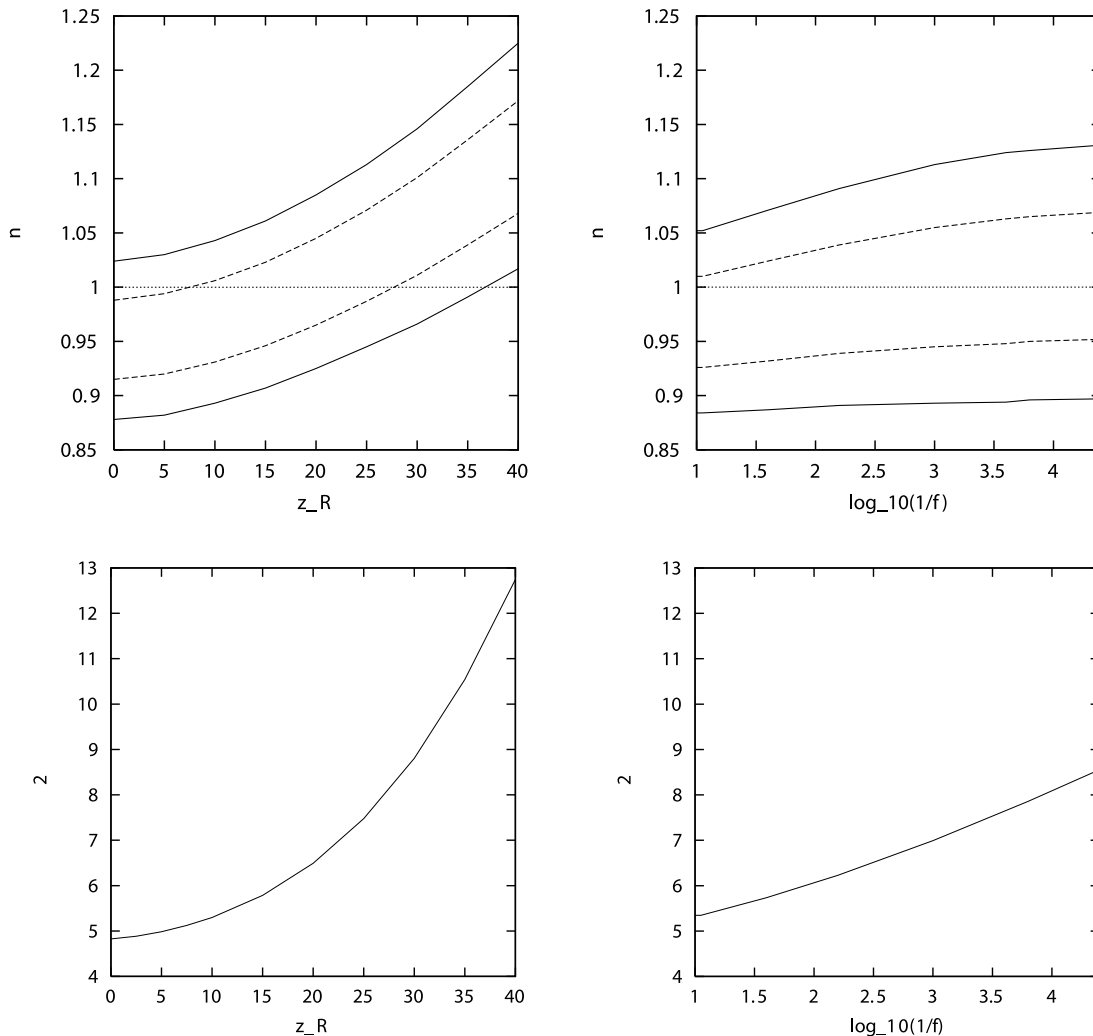


Figure 2. The top panels show nominal 1σ and 2σ bounds on n . In the left-hand panel the reionization epoch z_R is fixed. In the right-hand panel is fixed instead the fraction f of matter that is assumed to have collapsed when at the epoch of reionization. (The corresponding reionization redshift, at best fit, is in the range 10–26.) The bottom panels show χ^2 with three degrees of freedom.

value of n found by TZH01.⁵ It is interesting that the PSCz survey used by TZH01 is well-fitted by a relatively low value of $\bar{\Gamma}$, which corresponds more or less to the one produced by our global fit. This may indicate that the slope of the galaxy correlation function used by TZH01 is more accurate than the earlier estimate that we (and many other authors) used. Still, had TZH01 used $\bar{\sigma}_8$ as a data point, their best fit to the slope of the galaxy correlation function would have been higher, because of the correlation between the fitted value of that slope and the value of $\bar{\sigma}_8$. As a result their best-fitting value of n would have been higher. Probably, more significantly, it would have also been higher if they had used our procedure of making a realistic estimate of the reionization redshift, instead of allowing it to float. We shall see that our higher value of n becomes interesting, in the context of certain models of inflation suggested by the effective field theory.

⁵ Ignoring the differences in the other parameters, changing n from the TZH01 value to our value would raise the spectrum at $k^{-1} = 8 h^{-1} \text{ Mpc}$ by 9 per cent. Roughly speaking, this raises $\bar{\sigma}_8$ by the same amount, taking us from the TZH01 value 0.48 to a value 0.53 which is in reasonable agreement with the result of our fit.

3 MODELS OF INFLATION

3.1 The general framework

Our next objective is to compare the observational constraint on n with some models of inflation. Before going into the details, it will be useful to describe the general framework within which we operate, since it radically differs both from the ‘reconstruction’ programme (Lidsey et al. 1997) and from a proposed ‘small/large/hybrid’ classification of potentials (Dodelson, Kinney & Kolb 1997; Kinney et al. 2001).

Inflation is supposed to perform two separate jobs. One is to evolve the Universe from a generic initial condition at, presumably, the Planck scale, without either collapsing or becoming empty. The other is to set, after inflation is over, the initial conditions that describe the observable Universe, in particular the primordial curvature perturbation. The second job is done during the last 50 or so e-folds of inflation, while observable scales are leaving the horizon. To produce the nearly scale-invariant perturbation that we see, inflation during this era presumably has to be of the slow-roll variety, which implies that $\rho^{1/4}$ is at least a couple of orders of magnitude below the Planck scale [equation (4) below]. For our

purpose, a ‘model of inflation’ is a model of this era, which alone is accessible to observation.

At the most primitive level, a model of inflation is a form for the potential during inflation, and a specification of the field value at the end of slow-roll inflation. (In hybrid models, the field value at the end of slow-roll inflation is not determined by the form of the potential during inflation, because the end corresponds to the destabilization of some non-inflaton field.) At this primitive level, though, one has complete freedom in choosing the form of the potential during inflation, and consequently very little predictive power.⁶ In order to reduce the freedom, one therefore looks to the effective field theory for guidance.

Effective field theory provides the framework for the Standard Model of particle physics and for its phenomenological extensions. It is supposed to be valid on energy scales far below the ultraviolet cut-off Λ_{UV} , which is at most of the order of the Planck scale. In this regime, the unknown physics beyond the cut-off is ignored (in a renormalizable theory) or else encoded by the inclusion of the leading non-renormalizable term(s). In contrast, an attempt to use effective theory on scales approaching the cut-off would require an infinite number of non-renormalizable terms, leading to a complete loss of predictive power. In the present context, the relevant non-renormalizable terms are contributions to V of the form $\lambda_n \phi^{4+n}/\Lambda_{UV}^n$. A widely held view, which we adopt here, is that for a generic field the coefficients λ_n have magnitude of order one. In models based on effective field theory the non-renormalizable terms are essentially neglected, and, taking optimistically $\Lambda_{UV} \sim M_P$, this neglect then requires a generic field $|\phi| \ll M_P$.⁷ [Sometimes one forbids non-renormalizable terms in $V(\phi)$ by invoking a suitable symmetry, but according to current ideas this is likely to work only for a limited number of terms (Lyth & Riotto 1999; Stewart & Cohn 2000).]

Instead of effective field theory, one may hope to use a deeper theory like string theory, which would determine the coefficients of all of the non-renormalizable terms. Such a theory might predict that the coefficients of these terms are very small (in Planck units), making it easy to have inflation with very large field values. This approach does yield some proposals for the potential of moduli (Lyth & Riotto 1999; Banks, Dine & Motl 2001), perhaps leading to inflation with a potential of the form $V \simeq V_0 - \frac{1}{2}m^2\phi^2 + \dots$ (last row of Table 2) which would require a field variation of order M_P . [A different stringy proposal (Dvali & Tye 1999) does not lead to a viable model.] Apart from this exception, it seems that at the present time predictive models have to be based on effective field theory, in which the relevant values of the inflaton field are small on the Planck scale. We do not know whether nature has chosen this option, or has instead chosen inflation with large field values, but we consider that in the latter case there is, at present,

⁶ Even the relatively restrictive slow-roll paradigm presented below leads only to the gravitational wave constraint $r = -6.2n_T$ and the flatness conditions given by $ln - 1 \ll 8$, $ln_T \ll 2$.

⁷ In the usual case, that the real inflaton field ϕ is the radial part of some complex field, the origin $\phi = 0$ can be taken as the fixed point of the symmetries of the renormalizable field theory. If the inflaton field is the angular part (a pseudo-Goldstone boson) it runs over only a finite range, and its origin within this range is arbitrary. Irrespective of the definition of the origin, the neglect of non-renormalizable terms requires the *range* of ϕ spanned by relevant field values to be much less than Λ_{UV} , and most of the following discussion considers if this requirement replaces the assumption that ϕ itself is small. Note that the assumption of small ϕ is a minimal one, necessary to justify the neglect of non-renormalizable terms, but by no means always sufficient (Lyth & Riotto 1999).

Table 2. Predictions for the spectral index n , in terms of the number of e-folds N to the end of slow-roll inflation. Ignoring the slight scale dependence, $N = N_{COBE}$ is around 50 for the standard cosmology. For rows two and three there is a maximum amount of inflation, corresponding to N_{max} . All constants are positive, and p is an integer except for the mutated model. (The mutated model can also give a potential of the same form as ‘new’ inflation with any p bigger than 2.) In the top and bottom rows n can be far from 1, while in the other cases it is typically close to 1.

	$V(\phi)/V_0$	$\frac{1}{2}(n-1)$
Positive mass-squared	$1 + \frac{1}{2}\frac{m^2}{V_0}\phi^2$	$M_P^2 m^2/V_0$
Self interaction ($p \geq 3$)	$1 + c\phi^p$	$\frac{p-1}{p-2}\frac{1}{N_{max}-N}$
Dynamical symmetry breaking ($p \geq 1$)	$1 + c\phi^{-p}$	$\frac{p+1}{p+2}\frac{1}{N_{max}-N}$
Loop correction	$1 + c \ln \frac{\phi}{Q}$	$-\frac{1}{2N}$
Mutated ($-1 < p < \infty$)	$1 - c\phi^{-p}$	$-\left(\frac{p+1}{p+2}\right)\frac{1}{N}$
‘New’ ($p \geq 3$)	$1 - c\phi^p$	$-\left(\frac{p-1}{p-2}\right)\frac{1}{N}$
Negative mass-squared	$1 - \frac{1}{2}\frac{m^2}{V_0}\phi^2$	$-M_P^2 m^2/V_0$

no theoretical guidance as to the form of the potential. Hence we focus on effective field theory models.

3.2 Slow-roll inflation

Slow-roll inflation, with a single-component inflaton field, is described by the following basic set of formulae (Lyth & Riotto 1999; Liddle & Lyth 2000).⁸ In these formulae, ϕ is the inflaton field, and V is its potential during inflation. The other quantities are the Planck mass $M_P = 2.4 \times 10^{18}$ GeV, the scale factor of the Universe a , the Hubble parameter $H = \dot{a}/a$, and the wavenumber k/a of the cosmological perturbations. We assume the usual flatness conditions

$$\epsilon \ll 1, \quad |\eta| \ll 1, \quad (2)$$

$$\epsilon \equiv \frac{1}{2}M_P^2(V'/V)^2,$$

$$\eta \equiv M_P^2 V''/V,$$

leading to the slow-roll expression given by $3H\dot{\phi} \simeq -V'$.

The fundamental formula giving the spectrum of the curvature perturbation is

$$\frac{4}{25}\mathcal{P}_{\mathcal{R}}(k) = \frac{1}{75\pi^2 M_P^6} \frac{V^3}{V'^2}, \quad (3)$$

where the potential and its derivatives are evaluated at the epoch of horizon exit $k = aH$. On the scale k_{COBE} , the COBE normalization, equation (1), requires

$$V^{1/4} = 0.027 \epsilon^{1/4} M_P. \quad (4)$$

To work out the value of ϕ at the epoch of horizon exit, one uses

⁸ Multi-component models require a different treatment, as do the models in which slow-roll is briefly interrupted, and models with a quartic kinetic term (Armendariz-Picon, Damour & Mukhanov 1999). The inflaton field is supposed to be canonically normalized, which can always be achieved if the kinetic term has the usual quadratic form. Einstein gravity during inflation is assumed, which can usually be achieved by a conformal transformation even if the underlying theory is non-Einstein in nature.

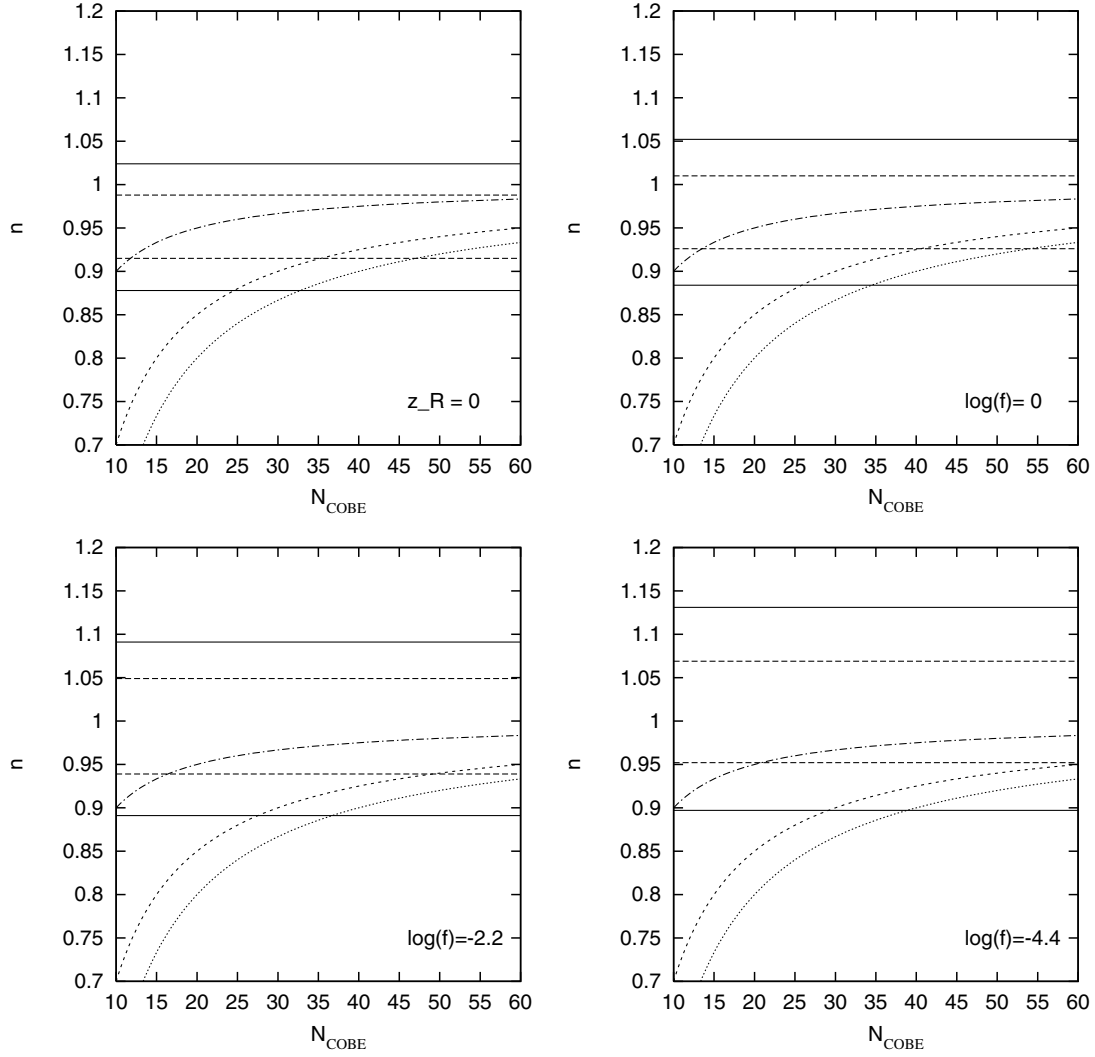


Figure 3. The horizontal lines show the 1σ and 2σ bounds on n , with different panels corresponding to different assumptions about the epoch of reionization. Also shown is the dependence of n on N_{COBE} , according to some of the models shown in Table 2. From top to bottom, these are the logarithmic potential, new inflation with $p = 4$, and new inflation with $p = 3$. Significant lower bounds on N_{COBE} are obtained for the new inflation models. Considered seriously, the 1σ bound would practically rule out the $p = 3$ model.

the relation

$$\ln(k_{\text{end}}/k) \equiv N(k) = M_{\text{P}}^{-2} \int_{\phi_{\text{end}}}^{\phi} (V/V') d\phi, \quad (5)$$

where $N(k)$ is actually the number of e-folds from horizon exit to the end of slow-roll inflation. The biggest scale of interest may be taken as k_{COBE}^{-1} , which using the definition in our earlier work (Lyth & Covi 2000) corresponds to $k_{\text{COBE}}^{-1} \approx 730 h^{-1} \text{Mpc}$. Observations of the smaller-scale CMB anisotropy and galaxy surveys probe smaller values, $k^{-1} \sim 10 h^{-1} \text{Mpc}$, corresponding to a change $\Delta N \approx 4$ to 5. At a given scale, N depends on the post-inflationary evolution of the scale factor, and using the *COBE* scale it is usefully written as

$$N_{\text{COBE}} \approx 60 - \ln\left(\frac{10^{16} \text{GeV}}{V^{1/4}}\right) - \frac{1}{3} \ln\left(\frac{V^{1/4}}{T_{\text{reh}}}\right) - N_0. \quad (6)$$

In this expression, T_{reh} is the re-heat temperature after inflation, and V is the potential at the end of inflation. The final contribution $-N_0$ (negative in all reasonable cosmologies) exhibits our ignorance about what happens between this re-heat and nucleosynthesis. In

conventional cosmology, with the relatively high inflation scale occurring in most of our models, one expects $N_{\text{COBE}} \sim 50$ to 60, but late entropy release from thermal inflation (Lyth & Stewart 1996) (or a low value of V) can make N_{COBE} much lower. In some of the inflation models that we shall consider, our bound on n will lead to a useful lower bound on N_{COBE} .

The spectral index n is defined by

$$n(k) - 1 \equiv \frac{d \ln \mathcal{P}_{\mathcal{R}}}{d \ln k}, \quad (7)$$

and is given by equations (3) and (5) as (Liddle & Lyth 1992)

$$n - 1 = 2\eta - 6\epsilon. \quad (8)$$

It defines the scale dependence of $\mathcal{P}_{\mathcal{R}}(k)$ leaving its value at (say) the *COBE* scale as the only other quantity required to specify it completely.

Finally, the spectrum of the primordial gravitational waves is characterized by its contribution r to the spectrum of the CMB anisotropy on the *COBE* scale (defined in a certain approximation and measured in units of the contribution of the curvature perturbation) and its spectral index n_{T} , which are given by (Liddle

Table 3. Fit of the Λ CDM model to presently available data. The scale-dependent spectral index is given by equation (14) with $c = 0.1$. Free parameters are $n_{\text{COBE}} = 1 + 2(s - c)$, and the next three quantities in the table. Reionization is considered to occur when a fraction $f = 10^{-2.2}$ of matter has collapsed. (The corresponding redshift at best fit is $z_R = 21$.) Every quantity except n_{COBE} is a data point, with the value and uncertainty listed in the first two rows. The result of the least-squares fit is given in lines three to five. All uncertainties are at the nominal 1σ level. The total χ^2 is 8.4 with three degrees of freedom.

	n_{COBE}	$\Omega_B h^2$	Ω_0	h	$\tilde{\Gamma}$	$\tilde{\sigma}_8$	C_{ℓ}^{1st}	$C_{\ell}^{\text{2nd}}/C_{\ell}^{\text{1st}}$
Data	—	0.019	0.35	0.65	0.23	0.56	74.0 μK	0.38
Error	—	0.002	0.075	0.075	0.035	0.059	5 μK	0.06
Fit	0.94	0.021	0.40	0.59	0.19	0.53	67.6 μK	0.49
Error	0.04	0.002	0.05	0.05	—	—	—	—
χ^2	—	0.9	0.4	0.6	1.2	0.2	1.6	3.5

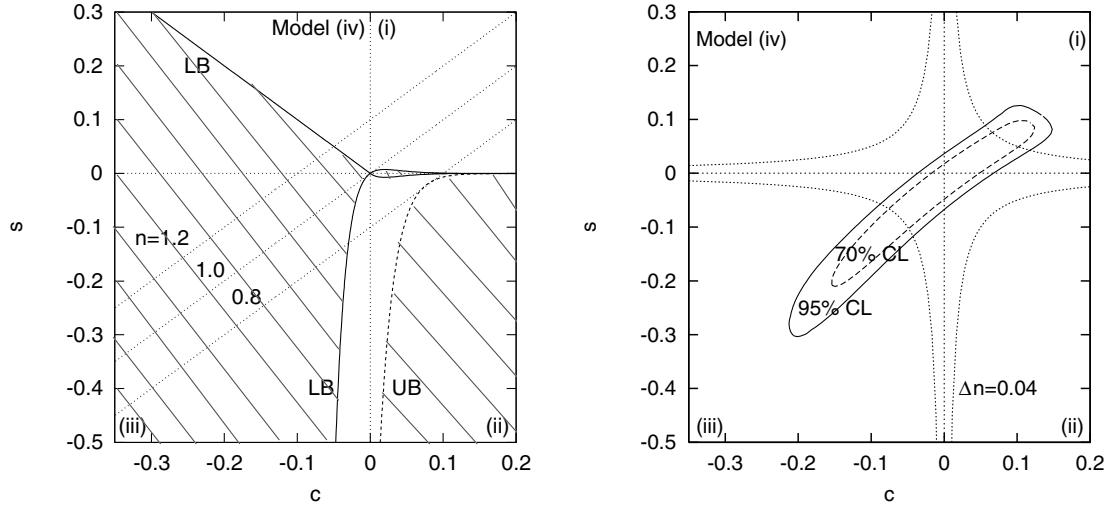


Figure 4. The parameter space for the running mass model. As discussed in Lyth & Covi (2000) the model comes in four versions, corresponding to the four quadrants of the parameter space. In the left-hand panel, the straight lines correspond to $n_{\text{COBE}} = 1.2, 1.0$ and 0.8 , and the hatched region is not favoured on theoretical grounds. In the right-hand panel, we show the region allowed by observation, in the case where reionization occurs when $f \sim 1$. To show the scale dependence of the prediction for n , we also show in this panel the branches of the hyperbola $8sc = \Delta n \equiv n_8 - n_{\text{COBE}}$, for the reference value $\Delta n = 0.04$.

& Lyth 1992)

$$r = 12.4\epsilon \quad (9)$$

and

$$n_T = -2\epsilon. \quad (10)$$

We are going to apply these slow-roll equations to models of inflation in which the relevant values of the inflaton field are small. Quite generally, such models predict that r is too small to be observed in the foreseeable future, in accordance with the assumption of our fit (Lyth 1997). Indeed, applying equation (5) to the range of scales $\Delta N \approx 4$ over which gravitational waves affect the CMB anisotropy, one finds that

$$\frac{r}{0.1} \sim \left(\frac{\Delta\phi}{0.5M_P} \right)^2, \quad (11)$$

where $\Delta\phi$ is the corresponding change in ϕ , and $r \approx 0.1$ is about the smallest signal that can be detected by the *Planck* satellite. A detectable signal therefore requires that the change in ϕ over relevant field values be large, and therefore that the value of ϕ itself be large for at least some relevant field values. We emphasize again that we have no idea of whether nature has chosen small

or large field values, and that we focus on the small-field case because in our view only that case is at present understandable from the point of view of effective field theory.

For future reference, we note that the converse of the above result does not apply. The total change in ϕ after the *COBE* scale leaves the horizon can be large in a model, where the change over the relevant four e-folds is small. As a result, large-field models do not necessarily lead to significant gravitational waves. For instance, if V depends linearly on ϕ , then $N(\phi) \propto \phi$, and the change in ϕ after the *COBE* scale leaves the horizon is related to the change $\Delta\phi$ during four e-folds by $\phi_{\text{COBE}}/\Delta\phi \approx N_{\text{COBE}}/4 \gg 1$.

3.3 Some simple models

Effective field theory, with non-renormalizable terms essentially ignored, allows only a few different types of terms for the variation of V . With the reasonable assumption that one such term dominates over the relevant range of ϕ , we arrive essentially at the models displayed in Table 2. Details of these models, with extensive references and possible complications, are given in Lyth & Riotto (1999). One of these complications is the possibility, considered by several authors, that two terms of the inflaton potential need to be kept over the relevant range of ϕ . While this can happen, the

dominance of one term is the generic situation in the sense that it holds over most of the parameter space of the potential.⁹

When the *COBE* normalization is imposed on the prediction, the requirement of small, values of the inflaton field can generally be satisfied with physically reasonable values of the parameters. An exception is the potential $V = V_0 - \frac{1}{2}m^2\phi^2 + \dots$, which requires $\phi \sim M_P$ at the end of inflation (see below). The only other significant exception is the logarithmic potential, which requires $\phi \sim M_P$ when cosmological scales leave the horizon, if the coupling is unsuppressed as in the case of *D*-term inflation.

Given the restriction on ϕ , the flatness conditions given by equation (2) require that V_0 dominates the potential in all of the models, leading to simple expressions for ϵ and η . The contribution of gravitational waves is negligibly small in all of them, and the formula for n is well approximated by

$$n - 1 = 2\eta. \quad (12)$$

The resulting prediction for n is shown in Table 2. Except in the first and last rows, the prediction depends on N and is therefore scale-dependent. However, since n is constrained to be close to one, the scale dependence is negligible over the cosmological range $\Delta N \sim 4$ (Lyth & Covi 2000), and accordingly one may set $N = N_{\text{COBE}}$. The bottom two rows correspond to single-field inflation with a mass term or a self-interaction dominating, and an unspecified term stabilizing the potential after inflation. The other rows correspond to hybrid inflation, where a non-inflaton field is responsible for most of the potential during inflation. The loop correction is the one which arises with spontaneously broken global supersymmetry, as for example in ‘*D*-term inflation’. The ranges of p are the ones in which the prediction for the spectral index holds, and they can be achieved in effective field theory with at most a single non-renormalizable term.

The strongest prediction comes from the models giving $n - 1 \propto 1/N$. It is shown in Fig. 3 for the three most popular versions of these models, along with the observational bounds on n . In the ‘new’ inflation models there is a non-trivial lower bound on N , which would almost exclude the $p = 3$ model if the 1σ bound were taken seriously.

Another case of interest is the potential $V = V_0 - \frac{1}{2}m^2\phi^2 + \dots$. More or less independently of the additional terms which stabilize the potential, the vacuum expectation value (vev) of ϕ is $\langle\phi\rangle \sim \sqrt{2V_0/m^2} = [2/(1-n)]^{1/2}M_P$. Depending on the nature of ϕ , this kind of inflation has been termed ‘natural’, ‘topological’ and ‘modular’ [see for instance Banks et al. (2001) for a recent espousal of modular inflation]. In all cases the model is regarded as implausible if $\langle\phi\rangle$ is much bigger than M_P , which means that it is viable only if n is not too close to 1. Our 2σ bound $n \geq 0.9$ implies $\langle\phi\rangle \geq 4.5M_P$, which may perhaps be regarded as already not favouring these models.

⁹ Consider, for instance, the case where there are just two parameters, corresponding to the overall normalization of the two terms. At a given field value, parameter space then consists of a region where one term dominates and a region where the other term dominates, these regions being divided by a line corresponding to 50 per cent of each term. If we consider the cosmological range of field values, and interpret the ‘dominance’ of one term as say a factor of 10 between them, the line becomes a band, but still a set of measure zero compared with all of parameter space. Finally, the *COBE* normalization corresponds to a line in the parameter space, which will generically cross the band; only very exceptionally will the line lie within the band. See for an example fig. 1 of Buchmüller, Covi & Delépine (2000), which shows for a specific model that the full potential is well approximated by a single term in the region of dominance.

3.4 Alternative views

The view we have taken is different from the one espoused in Dodelson et al. (1997) and Kinney et al. (2001). These authors consider the potentials in the first, second, third and last rows of Table 2 (and a linear potential) but unlike us they take such field-theoretic forms of the potential seriously even at $\phi \gtrsim M_P$. In particular, they consider the limit where the constant term is negligible, corresponding to monomial potentials like $V \propto \phi^2$ (Linde 1983).¹⁰ This procedure allows a significant gravitational wave contribution r , and a wide range of n for each r . Therefore, to delineate the allowed region of parameter space, Kinney et al. (2001) allow both n and r to vary. We, in contrast, consider only small field values, leading to negligible r which we set equal to zero. We consider that in the regime $\phi \gtrsim M_P$, a single-power form for the variation of ϕ is no more likely than any other, and therefore that the potentials in Table 2 have no special status in this regime.

While the assumption of a single power seems too restrictive, it might be reasonably argued that a combination of two or three powers (say positive integral powers) will be sufficiently flexible to cover a useful range of potentials. Why, then, in the large-field regime, do we not wish to focus in particular on the case that one power dominates, as we did for the small-field regime? Our answer illustrates beautifully the difference of view that we take in these two regimes. In the small-field regime, each power listed in Table 3 has a more or less definite physical origin; for instance, positive powers correspond to different self-coupling terms for the inflaton. In that situation, it seems reasonable to regard the coefficients of these powers as parameters which, in the present state of theory, have more or less equal prior probability. Then, over most of the parameter space (and even over most of the restricted region allowed by the *COBE* normalization) just one power dominates, making this the most likely situation. In the large-field case, on the other hand, we argue that a single power and the parameters of an expansion consisting of several powers have no special significance. Instead of single powers, one could choose a new basis consisting of linear combination of powers (e.g. Legendre polynomials instead of monomials) leading to new ‘parameters’ which would have to be chosen specially to reproduce a single power. This brings us back to the position stated earlier, that according to us there is no theoretical guidance for the form of the potential in the large-field regime.

Precisely this view provided the starting point of the ‘reconstruction’ programme reviewed in Lidsey et al. (1997). The idea here is that, if significant gravitational waves are observed, then equations (3), (8), (9) and (10), and more accurate versions (Stewart & Lyth 1993) involving one higher derivative of V , may allow V to be reconstructed over the very limited range of ϕ corresponding to horizon exit for cosmological scales. We have no comment on this purely phenomenological approach, except to emphasize that it works only if r is big enough to measure.

4 RUNNING MASS MODELS

We also considered the case of running mass inflation models,

¹⁰ With these particular examples in mind, they divide the n - r plane into regimes corresponding to $\eta < 0$, $0 < \eta < 2\epsilon$ and $2\epsilon < \eta$, labelling them respectively as the (non-hybrid) small-field, (non-hybrid) large-field and hybrid regimes. These designations do not have general validity, and indeed seem to be confined to the particular examples already mentioned.

which give a spectral index with potentially strong scale dependence. The potential in this case corresponds to a loop correction in the context of softly broken global supersymmetry, and is of the form

$$V = V_0 \left[1 + \frac{1}{p} c \phi^p \ln(\phi/Q) \right]. \quad (13)$$

The case $p = 2$ corresponds to a renormalizable interaction, which alone has been studied so far (Stewart 1997a,b; Covi 1999; Covi & Lyth 1999; Covi, Lyth & Roszkowski 1999; German, Ross & Sarkar 2000; Lyth & Covi 2000). It gives a spectral index of the form

$$\frac{n(k) - 1}{2} = s \exp[c \Delta N(k)] - c, \quad (14)$$

$$\Delta N(k) \equiv N(k_{\text{COBE}}) - N(k). \quad (15)$$

These models invoke the loop correction coming from softly, as opposed to spontaneously, broken renormalizable global supersymmetry. In the simplest scenario, c is essentially the coupling strength of the field in the loop, which is expected to be of the order of 0.1 to (say) 0.01 in the case of a gauge coupling.

Because of the possibly strong scale dependence of the curvature perturbation, our procedure of calculating the reionization redshift in terms of the fraction f of collapsed matter becomes crucial. The results are insensitive to f in the reasonable range of $f \gtrsim 10^{-4}$, which would not at all be the case if we fixed the reionization redshift instead.

In Fig. 4 we show the allowed region of parameter space with $f = 1$. We see that $c \sim 0.1$ is indeed allowed, and in Table 3 we show the result of a fit with c fixed at this value, with a central value of $f = 10^{-2.2}$. The corresponding CMB anisotropy and curvature spectrum are shown in Fig. 1. Comparing with the corresponding figures for the case of a scale-independent spectral index, the scale dependence generated by the coupling $c = 0.1$ is clearly visible. Although observations cannot yet clearly distinguish between the two cases, it is likely to do so in the future, deciding whether the inflaton has an unsuppressed coupling in this type of model. Note that, in contrast with the earlier fit (Lyth & Covi 2000), the maximum allowed value of n_{COBE} is now too small for overproduction of primordial black holes at the end of inflation (Leach, Grivell & Liddle 2000) to be a problem.

5 CONCLUSION

In continuation of our earlier work (Lyth & Covi 2000), we have fitted the Λ CDM model to a global data set, assuming that a Gaussian primordial curvature perturbation is the only perturbation present. The data set now includes heights of the first two peaks in the CMB anisotropy, derived from the Boomerang and Maxima data. We focus on the spectral index n , specifying the shape of the curvature perturbation, considering separately the case of a practically scale-independent spectral index, and the scale-dependent spectral index predicted by running mass inflation models. In contrast with other groups, we calculate the reionization epoch within the model on the assumption that it corresponds to the epoch when some fraction f of the matter collapses, the result being only mildly dependent on f in the reasonable range $f \gtrsim 10^{-4}$.

For the scale-independent case, the bounds on n are given in Fig. 3 for some typical values of f , and for the case of no reionization. In the same figure, the bounds are compared with the prediction of some forms of the inflationary potential which are

suggested by the effective field theory. The prediction depends on the number of e-folds N of inflation after cosmological scales leave the horizon, where $N \lesssim 60$ depends on the post-inflationary cosmology. For two of the models, the constraint on n rules out a significant portion of the n - N plane.

In the case of running mass models, the scale-dependent spectral index depends on parameters s and c , the latter being related to the inflaton coupling which produces the running. We have delineated the allowed region in the s - c plane. An unsuppressed coupling of $c \sim 0.1$ is allowed by the data, leading to a noticeable scale dependence of the spectral index. The fit with $c = 0.1$ is not as good as one with a scale-independent spectral index, but is still acceptable.

ACKNOWLEDGMENTS

We would like to thank A. D. Linde for useful comments on the first version of this paper.

REFERENCES

- Armendariz-Picon C., Damour T., Mukhanov V., 1999, Phys. Lett. B, 458, 209
- Bahcall N. A., Ostriker J. P., Perlmutter S., Steinhardt P. J., 1999, Sci, 284, 1481
- Banks M., Dine M., Motl L., 2001, JHEP, 0101, 031
- Buchmüller W., Covi L., Delépine D., 2000, Phys. Lett. B, 491, 183
- Covi L., 1999, Phys. Rev. D, 60, 023513
- Covi L., Lyth D. H., 1999, Phys. Rev. D, 59, 063515
- Covi L., Lyth D. H., Roszkowski L., 1999, Phys. Rev. D, 60, 023509
- de Bernardis P. et al., 2000, Nat, 404, 955
- Dodelson S., Kinney W. H., Kolb E. W., 1997, Phys. Rev. D, 56, 3207
- Dvali G., Tye S. H., 1999, Phys. Lett. B, 450, 72
- Freedman W. L., 2000, Phys. Scr., T85, 37
- German G., Ross G., Sarkar S., 1999, Phys. Lett. B, 469, 46
- Hanany S. et al., 2000, ApJ, 545, L5
- Jaffe A. H. et al., 2001, Phys. Rev. Lett., 86, 3475
- Kinney W. H., Melchiorri A., Riotto A., 2001, Phys. Rev. D, 63, 023505
- Leach S. M., Grivell I. J., Liddle A. R., 2000, Phys. Rev. D, 62, 043516
- Liddle A. R., Lyth D. H., 1992, Phys. Lett. B, 291, 391
- Liddle A. R., Lyth D. H., 1995, MNRAS, 273, 1177
- Liddle A. R., Lyth D. H., 2000, Cosmological Inflation and Large Scale Structure. Cambridge Univ. Press, Cambridge
- Lidsey J. E., Liddle A. R., Kolb E. W., Copeland E. J., Barreiro T., Abney M., 1997, Rev. Mod. Phys., 69, 373
- Linde A. D., 1983, Phys. Lett. B, 129, 177
- Lyth D. H., 1997, Phys. Rev. Lett., 78, 1861
- Lyth D. H., Covi L., 2000, Phys. Rev. D, 62, 103504
- Lyth D. H., Riotto A., 1999, Phys. Rep., 314, 1
- Lyth D. H., Stewart E. D., 1996, Phys. Rev. D, 53, 1784
- Olive K. A., Steigman G., Walker T. P., 2000, Phys. Rep., 333, 389
- Sarkar S., 1999, in Klapdor-Kleingrothaus H. V., Baudis L., eds, Dark Matter in Astrophysics and Particle Physics. IOP Publishing, Bristol, p. 108
- Saunders W. et al., 2000, MNRAS, 317, 55
- Stewart E. D., 1997a, Phys. Lett. B, 391, 34
- Stewart E. D., 1997b, Phys. Rev. D, 56, 2019
- Stewart E. D., Cohn J. D., 2000, Phys. Lett. B, 475, 231
- Stewart E. D., Lyth D. H., 1993, Phys. Lett. B, 302, 171
- Tegmark M., Zaldarriaga M., Hamilton A. J. S., 2001, Phys. Rev. D, 63, 043007 (TZH01)
- Turner M. S., 1999, in Caldwell D. O., ed., Cosmo-98. Am. Inst. Phys., New York, p. 113

This paper has been typeset from a \LaTeX file prepared by the author.